doi: 10.56761/EFRE2022.S4-O-027404

Operation of multi-gigawatt magnetic compression lines

S. Tsyranov[*]

Institute of Electrophysics UB RAN, Yekaterinburg, Russia
[*]*serg@iep.uran.ru*

Abstract. The paper presents the results of theoretical study the mechanism of Magnetic Compression Lines (MCL) operation in the multi-gigawatt power range. It has been found that the MCL regime is realized under the condition when the precession period of the magnetic moment is less than T_0, where T_0 is twice the propagation time of an electromagnetic wave between the inner and outer conductors of the line. The studies have shown that the input pulse amplification in power has its maximum value when an input pulse width is around of $4T_0$. While moving along the MCL, the input pulse splits in two peaks and then the energy is redistributed in favor of the first peak. This effect is due to the fact that several periods of precession are located within the first and second peaks, and their number and frequency change during the movement.

Keywords: Magnetic Compression Line, multi-gigawatt power, Landau Lifshitz equation.

1. Introduction

Non-linear transmission lines (NLTL) filled with saturated ferrite are used as solid-state sources of high-power microwave oscillations [1]. Application of a pulse magnetic field orthogonal to bias constant magnetic field in time less than the relaxation time, leads to the precession of the magnetic moment vector and generation of voltage oscillations across the NLTL output. Recently NLTLs also have been used to increase the peak power of picosecond unipolar pulses in the multi-gigawatt power range [2, 3]. Such kind of NLTLs is called Magnetic Compression Line (MCL). Shortening the duration of the input voltage pulse made it possible to obtain only one oscillation at the line output instead of several oscillations. The highest peak power achieved with the MCL is 77 GW with the voltage amplitude of 1.93 MV and pulse duration of 105 ps [3]. In this paper, the mechanism of MCL operation is numerically and analytically studied.

2. Model

The simulation was carried out using the Maxwell equations (1) and the Landau-Lifshitz equation (2), which describe the dynamics of the electromagnetic field and magnetization, respectively.

$$\begin{aligned} \frac{\partial\left(\varepsilon\cdot\varepsilon_0\cdot E\right)}{\partial t} &= c\cdot\eta_0\cdot\nabla\times H \\ \frac{\partial B}{\partial t} &= -\frac{c}{\eta_0}\cdot\nabla\times E \end{aligned} \tag{1}$$

where c – speed of light, $\eta_0 = \mu_0\cdot c$ – impedance of free space, ε_0, μ_0 – magnetic and electric constants, E – electric field vector [B/m], H, B и M – vectors of the magnetic field, magnetic induction and magnetization, respectively. For the convenience of calculations (1) are written in the form where the values of H, M and $B = H + M$ are expressed in the same units [A/m].

$$\frac{\partial M}{\partial t} = \gamma\cdot\mu_0\cdot\left[M\times H\right] - \alpha\cdot\frac{\gamma\cdot\mu}{M_s}\cdot\left[M\times\left[M\times H\right]\right] \tag{2}$$

where γ – gyromagnetic ratio for an electron α – phenomenological coefficient damping, M_s – saturation magnetic moment. It is convenient to represent the equations in a cylindrical coordinate system (r, θ, z). Assuming uniformity in angle θ, we can proceed to a two-dimensional problem in coordinates (r, z) (Fig.1). The simulation was carried out by the FDTD (Finite Difference Time

Domain) method using the YEE scheme with PEC (perfect electric conductor) boundary conditions on the inner and outer diameters of the line and Brown's boundary conditions on the ferrite [7].

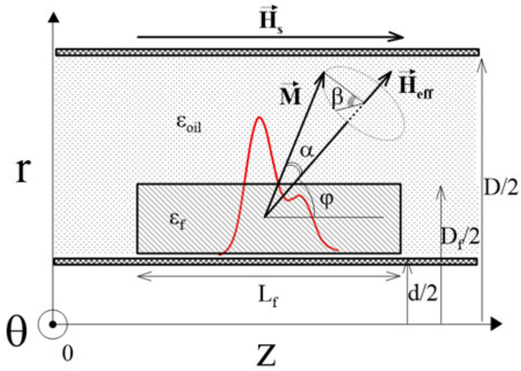

Fig.1. The geometry of the coaxial line with ferrite filling. The area filled with lines corresponds to ferrite with permittivity ε_f, dots – oil with ε_{oil}. The axis θ is perpendicular to the plane of the figure.

The boundary conditions at $Z = 0$ is set by the TEM wave entering the coaxial line and determining $E_r(r, t)$ and $H_\theta(r, t)$. Equation (2) was solved by the 4th order Runge-Kutta method. The geometry of the calculation model is shown in Fig.1 and corresponds to the parameters of the MCL4 line in the experiments [3]: $D/D_f/d$ = 22/12/8 mm, ferrite length L_f = 350 mm. In the calculations, the permittivity of the ferrite and transformer oil were $\varepsilon_f = 12$ and $\varepsilon_{oil} = 2.25$, respectively, the magnetic field of the solenoid was H_s = 106 kA/m, and the saturation magnetic moment of the ferrite (NiZn) determined by it was taken to be M_s = 300 kA/m. The phenomenological coefficient $\alpha = 0.05$ in (2) was used as a fitting factor to achieve the best agreement with the experiment.

3. Simulation results

Consider a simulation of the process of passage of a voltage pulse through a coaxial line with ferrite, the parameters of which are described above. The pulse had a sinusoidal shape with an amplitude of 1.5 MV and a base width of 400 ps, which is close to those used earlier in the experiment [3]. At a distance of 50 mm from the beginning of the ferrite, the pulse splits into two, and at a distance of 100 mm, into three peaks (Fig.2). The amplitude of the first peak continuously increases, while the second and third decreases. The change in energy of the first and second peaks are shown in Fig.3. Before the penetration of the voltage pulse into the ferrite, the constant field of the solenoid H_s created magnetization in it, while the angles α, φ, β in Fig.1 were equal to zero. The voltage pulse corresponds to a TEM wave with field components $\underline{E_r}$ and H_θ. When moving along the ferrite, the TEM wave field changes the field and the magnetization in the ferrite. The magnetic field corresponding to the voltage pulse can be estimated from the formula:

$$H_\theta = \frac{U}{2 \cdot \pi \cdot r \cdot Z_0} \tag{3}$$

where Z_0 = 40 Ohm – line impedance. Taking the average value of the pulse voltage U = 1.5/2 MV and the radius of the ferrite ring r = 5 mm, we obtain H_θ = 637 kA/m. The total magnetic field $H_\Sigma \approx H_\theta + H_z$ deviates from the line axis by an angle φ ~ 80° (Fig.1):

$$\cos(\varphi) \approx \frac{H_s}{H_s + H_\theta} \tag{4}$$

Under the action of a magnetic field, the ferrite magnetization, without changing modulo $M = M_s$, changes in direction, deviating from the line axis. Due to inertia, the process of magnetization change lags behind the change in the magnetic field. In the calculation, the angle between the magnetization M and the magnetic field H (α on Fig.1) at the pulse front increases from 0 to 22°, and then decreases to a value of 12°, which varies slightly further within the pulse.

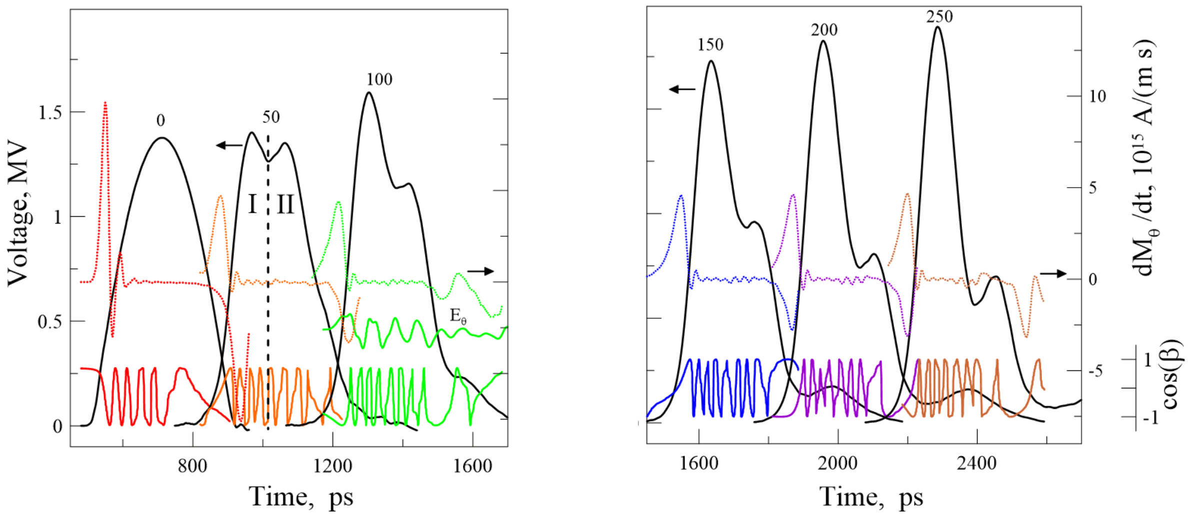

Fig.2. Dependences of voltage (black solid curves), cosine of the precession angle (solid color curves) and time derivative of the magnetization component M_θ (dot color curves) in sections of a ferrite with coordinates shown by numbers above the curves (0, 50, 100, 150, 200 and 250 mm) from time. The dashed line separates regions I and II related to the first and second voltage peaks. The time dependence of the field component E_θ with an amplitude of 3 MA/m in a section with a coordinate of 100 mm is shown.

At a non-zero angle, the precession of the vector M around the vector H occurs, the precession angle β continuously increases (cos(β) on Fig.2). When the orientation of the vector M changes, the value of the magnetic flux through any fixed circuit changes, which causes the appearance of electric induction fields in the circuit. It follows from the second equation in (1) that the value of the electric field E_r and E_z is affected by the rate of change of the magnetization component M_θ, and the value E_θ is affected by the rate of change M_r and M_z. For the process of transformation of the voltage pulse, the determining factor is the influence of the precession of the magnetization vector on E_r. The precession of the magnetization vector generates a magnetic wave in the ferrite, which will be referred to below as a magnetostatic wave (MSW). In the process of moving along the ferrite, there is a mutual change in MSW and voltage pulse (Fig.2). Let us write down the projections of the magnetization vector M on the coordinate axes (Fig.1):

$$\begin{aligned} M_r &= M_s \cdot \sin(\alpha) \cdot \sin(\beta) \\ M_\theta &= M_s \cdot (\sin(\alpha) \cdot \cos(\varphi) \cdot \cos(\beta) + \cos(\alpha) \cdot \sin(\varphi)) \\ M_z &= M_s \cdot (\sin(\alpha) \cdot \sin(\varphi) \cdot \cos(\beta) + \cos(\alpha) \cdot \cos(\varphi)) \end{aligned} \tag{5}$$

Assuming that the angle β changes with frequency ω, we write the rate of change M_θ:

$$\frac{dM_\theta}{dt} = -M_s \cdot \sin(\alpha) \cdot \cos(\varphi) \cdot \sin(\omega \cdot t) \cdot \omega \tag{6}$$

As can be seen from Fig.2, the amplitude dM_θ/dt outside the voltage pulse and in the region of the voltage pulse differ by more than an order of magnitude. This is due to the large difference in the value of the voltage, and hence the magnetic field that determines the angles α, φ in (6). Note that when the amplitude of the voltage pulse decreases by 5–10 times to values corresponding to the classical oscillation generation mode [1], the amplitude dM_θ/dt before the voltage pulse and in the region of the voltage pulse become comparable. By integrating (1) one can obtain the one-dimensional telegraph equation [5]:

$$\frac{\partial U}{\partial z} = -L_0 \cdot \frac{dI}{dt} - \mu_0 \cdot \frac{(D_f - d)}{2} \cdot \frac{dM_\theta}{dt} \tag{7}$$

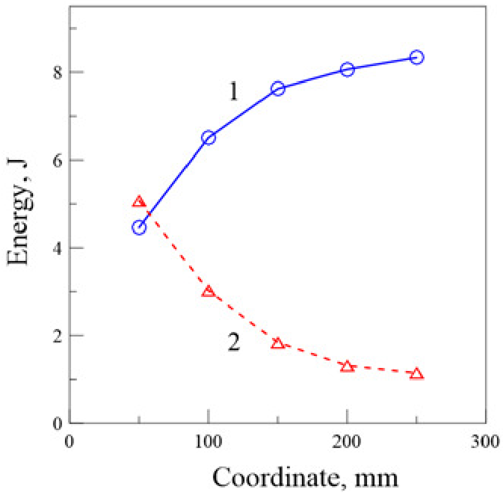

Fig.3. Energy of the first (1, solid curve) and second (2, dashed curve) peaks depending on the coordinate in the ferrite.

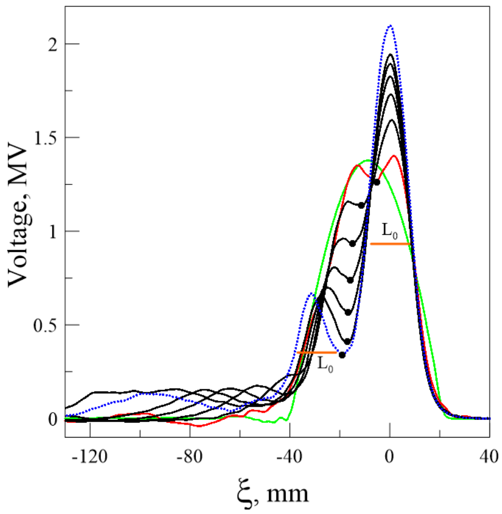

Fig.4. Dependences of voltage on the coordinate ξ in the coordinate system moving with of the voltage pulse speed. Dependencies are taken from the beginning of the ferrite (solid green curve) to its end (dotted blue curve). $V_f \sim 0.1533$ mm/ps, $\xi = z - V_f \cdot t$, $L_0 = V_f \cdot T_0$.

As can be seen from (7), the influence of the magnetization precession on the voltage pulse is significant in regions with a large value of dM_θ/dt, that is, at the boundaries of the voltage pulse (Fig.2). It seems that there is one "combined" period of magnetization precession in the region of the voltage pulse, which is similar to the classical mode of oscillation generation, where there is one period of precession per voltage pulse [1, 4]. However, the precession of the magnetization vector in the inner regions of the voltage pulse, despite its smallness dM_θ/dt, has a significant effect on the oscillation generation process. Using (6), we write the condition that the voltage derivative with respect to the coordinate is equal to zero in (7) as:

$$L_0 \cdot \frac{U_i}{Z_0} \cdot \omega_i \cdot \cos(\omega_i \cdot t) - \mu_0 \cdot \frac{(D_f - d)}{2} \cdot M_s \cdot \sin(\alpha) \cdot \cos(\varphi) \cdot \omega \cdot \sin(\omega \cdot t) = 0\,, \tag{8}$$

where U_i, ω_i are the amplitude and frequency of the input voltage pulse. Under the calculation conditions, equation (8) has three solutions in the vicinity of the point, the distance of which to the $U_i/2$ point is $t \sim 100$ ps ($L_0 \sim 15$ mm in the Fig.4). This is the reason for the formation of the second and then the third peaks in the region of the voltage pulse (Fig.2, Fig.4). Note that the value $t \sim 100$ ps is equal to the twice propagation time of an electromagnetic wave between the inner and outer diameters of the line T_0:

$$T_0 = \frac{D - D_f}{c} \cdot \sqrt{\varepsilon_{oil}} + \frac{D_f - d}{c} \cdot \sqrt{\varepsilon_f} \tag{9}$$

When a voltage pulse moves along the ferrite, the point where the derivative of voltage with respect to coordinate is zero, which separates the region of the first and second peaks, shifts relative to the pulse front (circles in the Fig.4) The width of the first and second peaks is always greater than L_0 which corresponds to a time equal to T_0. Then, according to the same mechanism, the third peak is formed in the region of the second peak, which reduces the energy in the region of the second peak.

For further analysis of the calculation results, let us consider the MSW characteristics in more detail. Let us consider the dependence of the frequency ω on the wave number k for magnetization waves in ferrite [6]:

$$k = \frac{\omega}{V_e}\left(\frac{\omega_2^2 - \omega^2}{\omega_1^2 - \omega^2}\right)^{1/2}, \tag{10}$$

$V_e = 1/(L_0 \cdot C_0)^{1/2}$, ω_1 and ω_2 – characteristic frequencies, which are determined by the geometry of the ferrite and the magnetic field value, and take values of ~14.15 10^{10} rad/s and ~14.19 10^{10} rad/s, respectively. Dispersion dependence (10) built on Fig.5 is divided into two branches: low-frequency acoustic (MSW) and high-frequency optical (OW). The speed of the TEM wave, that is, the speed of the voltage pulse, can be compared with the speed of the magnetic wave only on the acoustic branch at the point (ω_0, k_0), corresponding to the MSW wave with a period of 44 ps.
According to [4], the condition of synchronism of TEM and MSW waves (11) is satisfied at the frequency ω_0:

$$\omega_0 = \gamma \cdot \mu_0 \cdot H_\theta \cdot \sqrt{1 + \frac{\chi \cdot M_S}{\mu_0 \cdot H_\Sigma}}, \tag{11}$$

where χ =0.19 – is the filling factor of the line with ferrite $H_\Sigma \approx H_\theta + H_z$. For our calculation w_0 = 14 rad/s, which corresponds to a wave with a period of 44 ps and is consistent with the result. The precession period at the leading edge of the voltage wave varies from 39 to 26 ps (Fig.2), which turns out to be close to this value. When the speed of movement of the voltage pulse and the speed of MSW coincide, they move, exchanging energy synchronously. This is the first condition for the occurrence of oscillations [4]:

$$V_{ph} = V_f \tag{12}$$

The transfer of energy by a wave occurs with a group velocity. Accordingly, the transfer of energy from the pulse front along the magnetic wave occurs at a rate equal to the difference between the phase and group velocities. This speed difference must be positive, which corresponds to the second condition for oscillation excitation [4]:

$$V_{ph} > V_g \tag{13}$$

Fig.6 shows the dependences of the phase and group velocity of MSW waves on frequency plotted using (11). It can be seen that condition (13) is always satisfied, and the value of (V_{ph}-V_g) strongly depends on the frequency. In the process of moving along the ferrite, the oscillation period of the MSW wave in the region of the first and second peaks takes on the value of 38 and 43 ps at z = 50 mm and 28 and 90 ps at z = 250 mm (Fig.2). Due to the large difference in frequencies, the rate of energy supply to the region of the first peak turns out to be much higher than that of the second one (curve 3, Fig.6). With a decrease in amplitude, the speed of movement decreases the second peak lags behind the pulse front (Fig.4), therefore, the amount of energy entering the second peak region decreases.

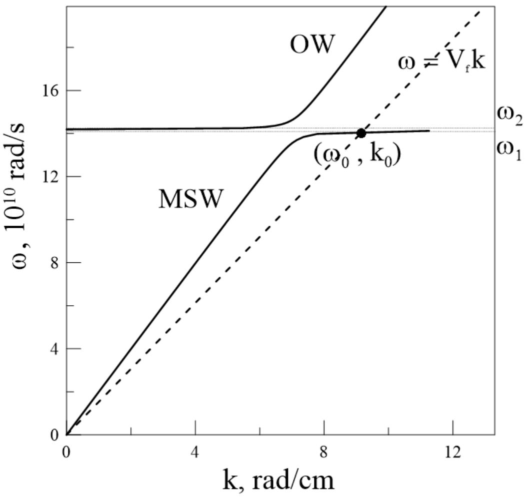

Fig.5. Dispersion relation of the magnetic waves (solid curves) and TEM wave (dash curve) in ferromagnetic media. OW: optical waves, MSW: magnetostatic waves. TEM wave speed – $V_f = c\cdot(\varepsilon_{eff}\cdot \mu_{eff})^{-1/2}$ ~ 1.533 10^{10} cm/s.

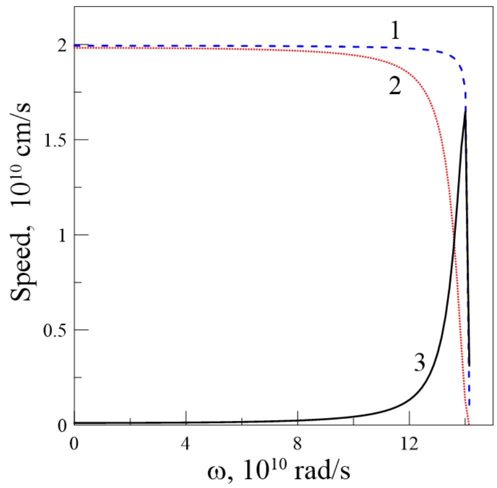

Fig.6. Phase velocity V_{ph} (dash blue curve), group velocity V_g (red dot curve), and velocity difference (V_{ph}–V_g) (black solid curve) for magnetostatic waves.

In addition to TEM, the calculation also revealed a superior wave of the H_{01} (TE_{01}) type. A wave of type H_{01} can exist in a coaxial waveguide if its length is less than the critical wavelength equal to the difference between the outer and inner diameters of the line. Critical wave period:

$$T_k = \frac{D-d}{V_f} \tag{14}$$

Fig.2 shows the component E_θ of the H_{01} wave, whose oscillation period ~70 ps is less than $T_k = 93$ ps (14), which satisfies the condition for the existence of the H_{01} wave. We associate the occurrence E_θ with the time derivatives of the components of the magnetization vector M_r and M_z. The magnetization components and their derivatives change with a precession period T_{pr} ~ 35 ps, creating an H_{01} wave component E_θ with an oscillation period of ~$2T_{pr}$ (Fig.2). The condition $T_{pr} < T_k$, necessary for the generation of wave H_{01}, is satisfied in the calculation with a margin. So, when a voltage pulse moves in a ferrite, there are three types of waves: the TEM wave of the voltage pulse, the magnetic wave MSW and the superior wave H_{01}.

4. Effect limits

An essential feature of the oscillation generation mechanism is that the period of precession of the magnetization vector is less than twice the propagation time of an electromagnetic wave between the inner and outer diameters of the line T_0 (9):

$$T_{pr} < T_0 \tag{15}$$

Note that when this condition is satisfied, there are several precession periods in the region of the voltage pulse. We can rewrite (11) approximately as:

$$\omega_0 \approx \gamma \cdot \mu_0 \cdot H_\theta \tag{16}$$

Using (3) and (16), we obtain the formula for the precession period in (ps):

$$T_{pr} \approx 180 \cdot \frac{r \cdot Z_0}{U} \tag{17}$$

where r is the average radius of the ferrite ring (m), Z_0 is the line resistance in the ferrite region (Ohm), U is the voltage amplitude (MV). Using (9), (17), (13) and the results of experiments [2, 3] fill in Table 1. As can be seen from the Table 1, condition (14) is satisfied for all previously performed experiments [2]. Note that the width of the output voltage pulse T_i is greater than T_0.

Table 1. MCL parameters.

Line	parameters						
	***U*, MV**	***D/d*, mm**	***D$_f$/d$_f$*, mm**	***r*, mm**	***T*$_{pr}$, ps**	***T*$_0$ (*T*$_k$), ps**	***T*$_i$, ps**
MCL4	1.93	22/8	12/8	5	23	96(93)	100
MCL3	1.48	38/14	24/16	10	61	172(160)	180
MCL2	1.12	101/37	65/40	26	221	483(433)	590
MCL1	0.74	275/102	180/110	72.5	881	1323(1153)	2100

***U и T_i** – amplitude and width of the voltage pulse at the line output

Using (9) and (17), we rewrite condition (14) as:

$$180 \cdot \frac{(D_f + d) \cdot Z_0}{2 \cdot U} < \frac{D - D_f}{c} \cdot \sqrt{\varepsilon_{oil}} + \frac{D_f - d}{c} \cdot \sqrt{\varepsilon_f} \tag{18}$$

we obtain the following expression:

$$U > \frac{0.045 \cdot Z_0 \cdot c \cdot (\gamma + 1/\alpha)}{(1-\gamma)\sqrt{\varepsilon_{oil}} + (\gamma - 1/\alpha)\sqrt{\varepsilon_f}} \ , \tag{19}$$

Where $\gamma = D_f/\mathrm{D}$, $\alpha = \mathrm{D}/d$. The smallest value of U is achieved at $\gamma = 1$, that is, when the space between the inner and outer diameters of the coaxial line is completely filled with ferrite:

$$U_{\min} \simeq \frac{0.045 \cdot Z_0 \cdot c \cdot (\alpha + 1)}{(\alpha - 1)\sqrt{\varepsilon_f}} \tag{20}$$

Calculation according to (20) for $Z_0 = 40$ Ohm gives 0.293 MV. Since a more complete implementation of the mechanism described above requires at least two precession periods within T_0, the threshold voltage required to fulfill condition (14) will be higher, on the order of ~0.6 MV.

5. Influence of the input pulse width

To study the influence of the input pulse width on the output pulse, a series of calculations was carried out, where the amplitude of the input sinusoidal pulse is fixed at 1.5 MV, and its base width varies within 100–500 ps. The calculation results are shown in Fig.7. It can be seen that a change in the width of the input pulse drastically changes the parameters of the output pulse. Note that the width at half height is 2/3 of the width at the base. For curve 1 in Fig.7, the input pulse width at half-height 67 ps is less than $T_0 = 93$ ps, respectively, the amplitude of the output pulse drops strongly, since its energy is spent on generating superior waves. Curve 2 shows the case when the pulse width at half maximum 133 ps is only slightly larger than T_0. At a small distance from the entrance to the ferrite, a soliton-like pulse is formed, which then moves without changing its shape (dashed curve 2 in Fig.7). The amplitude and width of the pulse differ little from the input pulse. Curves 3–5 demonstrate the variants when the width of the input pulse is sufficient for the formation of two or even three voltage peaks. The process mechanism has been described above.

An input pulse with a base width of 400 ps (~ $4T_0$) is optimal in the sense that, in the output pulse, the portion of the output pulse energy in the region of the first peak is maximum.

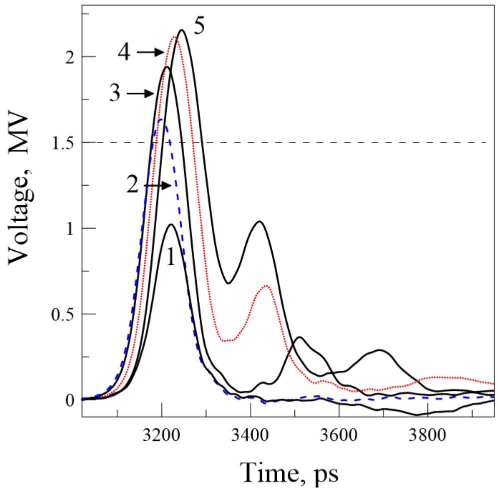

Fig.7. Time dependence of the output voltage for voltage pulses at the input to the line with an amplitude of 1.5MV and a base width of 1 – 100 ps, 2 – 200 ps, 3 – 300 ps, 4 – 400 ps, 5 – 500 ps.

6. Conclusion

In this paper, we numerically and analytically investigated the mechanism of generation of multi-gigawatt megavolt pulses in a coaxial line partially filled with ferrite. It has been established that for the implementation of the mechanism, it is necessary that the precession period of the magnetization vector T_{pr} be less than the value T_0, which is equal to twice the time of the electromagnetic wave travel between the inner and outer diameters of the line. It is shown that in order to fulfill such a condition, it is necessary that the amplitude of the input voltage pulse exceed 0.6 MV. Theoretical analysis and comparison with previous experiments made it possible to show that the width of the generated voltage pulses at the line output is limited by T_0. Studies have also shown that the amplification of the input pulse power is maximum at an input pulse width of ~$4T_0$. An essential feature of the mechanism is that in the process of moving along the line, the input pulse splits in two and then the energy is redistributed in favor of the first peak. In particular, this is due to the fact that several precession oscillations are located within the first and second peaks, and their number and frequency change during movement.

7. References

[1] Gubanov V.P., Gunin A.V., Kovalchuk O.B., Kutenkov V. O., Romanchenko I.V., Rostov V.V., *Technical Physics Letters,* **35**(7), 2009; doi: 10.1134/s1063785009070116N

[2] Alichkin E.A., Pedos M.S., Ponomarev A.V., Rukin S.N., Timoshenkov S.P., Karelin S.Y., *Review of Scientific Instruments* **91**, 104705, 2020; doi: 10.1063/5.0017980

[3] Rukin S., et al., *7th International Congress on Energy Fluxes and Radiation Effects (EFRE)*, Tomsk, 2020, pp. 92–97; doi: 10.1109/EFRE47760.2020.9241919

[4] Romanchenko I.V., et al., *Journal of Applied Physics*, **117** (21), 224102–681, 2015; doi: 10.1063/1.4922280

[5] Bolton, H.R., Dolan, J.E., *IEEE Proc.-Sci. Meas. Technol.*, **147**(5), 2000; doi: 10.1049/ip-smt:20000447

[6] Leblond H., *J. Phys. B: At. Mol. Opt. Phys.*, **41**, 043001, 2008; doi: 10.1088/0953-4075/41/4/043001

[7] Inan, U.S., Marshall, R.A., *Numerical Electromagnetics: The FDTD Method* (New York: Cambridge University Press, 2011).